Pb-induced skyrmions in a double layer of Fe on Ir(111)

Jonas Sassmannshausen, André Kubetzka,* Pin-Jui Hsu,† Kirsten von Bergmann,‡ and Roland Wiesendanger
Department of Physics, University of Hamburg, 20355 Hamburg, Germany

(Received 27 June 2018; revised manuscript received 2 October 2018; published 30 October 2018)

Spin-polarized scanning tunneling microscopy reveals that the spin-spiral period of a two-atomic-layer-thick Fe film on Ir(111) roughly doubles upon covering the system with a monolayer of Pb. The spin spirals have a zigzag shape and are guided by structural dislocation lines. In contrast to the spin spiral in the bare Fe double layer, the magnetic state of the Pb-covered Fe film responds to an external magnetic field: the spin spiral breaks up into segments, reminiscent of the spin-spiral state in the Fe triple layer on Ir(111), where the external magnetic field induces magnetic skyrmions. This demonstrates that the tuning of noncollinear spin textures is not only possible by interface engineering based on transition metals, but also with other metallic adlayers such as Pb with a filled *d* shell.

DOI: 10.1103/PhysRevB.98.144443

I. INTRODUCTION

In recent years, a lot of research effort has been invested into the search for materials hosting magnetic skyrmions. These magnetic quasiparticles are localized whirls in the magnetization, which are stabilized against collapse by the Dzyaloshinskii-Moriya interaction (DMI) [1–4]. They are often induced by external magnetic fields out of a spin-spiral ground state [5,6]. Such spin spirals typically result from a competition of ferromagnetic exchange interaction and strong DMI; the latter favors an orthogonal alignment of adjacent magnetic moments and in addition imposes a unique rotational sense. DMI can arise due to spin-orbit coupling in systems with broken inversion symmetry, such as chiral bulk crystals [5,6], but also at surfaces or interfaces [2]. The interplay of the magnetic interactions determines the nature of the magnetic ground state. To find materials that exhibit spin spirals and skyrmions with beneficial properties, a detailed knowledge of how to fine tune magnetic interactions is desirable.

The magnetic ground state of thin films is strongly dependent on the interfaces, a fact which is exploited in recent material-based research for skyrmions in magnetic multilayer systems [7–9]. One interface with a particularly strong DMI is Fe/Ir(111) [10], and the ground state of an Fe monolayer on Ir(111) is a nanoskyrmion lattice with about 13 atoms per skyrmion [10,11]. Based on this interface, a tuning of the magnetic state has been demonstrated by incorporating H atoms [12] or by covering the Fe with transition-metal overlayers. In particular, a Pd overlayer results in a spin-spiral ground state with a period of about 6 nm, out of which skyrmions can be induced by applied magnetic fields [13]; a Rh overlayer induces 1.0–1.5 nm one-dimensional magnetic states [14]; a Ni overlayer leads to a ferromagnetic ground state [15]; additional Fe layers result in spin spirals with periods of about 1.5 nm for the Fe double layer (Fe-DL) [16] and 3–10 nm for the Fe triple layer (Fe-TL) [17,18]; the latter exhibits skyrmions in applied magnetic fields.

In the present work, we choose Pb as an overlayer material and investigate its impact on the spin-spiral state of the Fe-DL on Ir(111). Lead is an element with large spin-orbit coupling, making it a candidate also for large DMI when interfaced with a magnetic layer. It has a filled *d*-electron shell, which might give rise to very different hybridization with the 3*d* magnetic transition-metal Fe, compared to the previously studied 3*d* and 4*d* overlayers [13–18]. Finally, Pb is superconducting below its critical temperature of 7.2 K. An interface between a magnetic film with noncollinear spin texture and one with superconductivity is believed to exhibit exotic behavior regarding both modifications of the spin polarization in the magnet as well as the properties of the superconductor, e.g., induced topological superconductivity [19,20].

II. EXPERIMENTAL DETAILS

We used (spin-polarized) scanning tunneling microscopy (SP-STM) [2,21] for the investigation of the structural and magnetic properties of our samples. The experiments were performed in ultrahigh vacuum (UHV; base pressure in the low 10^{-10} mbar range) at a measurement temperature of 4.2 K. The UHV system includes separate chambers for sample cleaning, material deposition, and STM measurements. The Ir(111) substrate was cleaned by cycles of 800 eV Ar-ion sputtering at room temperature for 20 min, at an Ar pressure of about 8×10^{-5} mbar, with subsequent annealing at a temperature of about 1600 K for 90 s. During Fe deposition, the sample was heated to about 330 °C. The Fe deposition rate was about 0.5 atomic layers (AL) per min. Because room-temperature growth of Pb results in intermixing of the Pb with the Fe film, in this work the Pb deposition was performed in a cooling stage with the sample held at a temperature of about 140 K. About 0.5–0.9 AL of Pb were

*kubetzka@physnet.uni-hamburg.de
†Present address: Department of Physics, National Tsing Hua University, 30013 Hsinchu, Taiwan.
‡kbergman@physnet.uni-hamburg.de

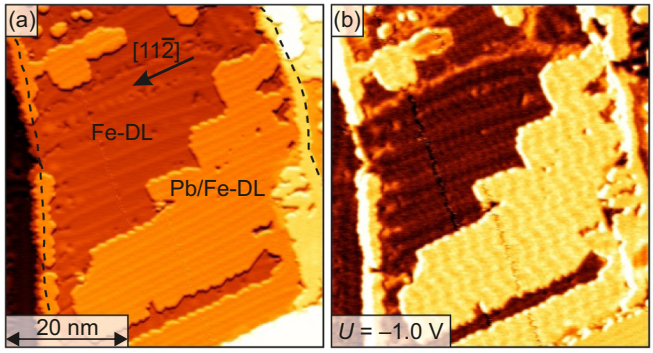

FIG. 1. SP-STM measurement of Pb on Fe on Ir(111). (a) Partially differentiated topography. An elongated Pb island on the Fe-DL is labeled, and buried step edges of the Ir substrate are indicated by dotted lines. (b) Simultaneously measured dI/dU map. Note that the line perpendicular to the dislocation lines on both the Fe-DL and the Pb/Fe-DL is an artifact of the digital feedback loop. $U = -1$ V, $I = 1$ nA, $T = 4.2$ K.

deposited onto the Fe/Ir(111) sample with a rate of roughly 3 AL per hour. STM topography images were measured in constant-current mode, and maps of the differential conductance (dI/dU) were recorded simultaneously using a lock-in amplifier. Electrochemically etched chromium bulk tips without further treatment were used for the presented spin-resolved measurements.

III. EXPERIMENTAL RESULTS

The topography of a typical sample of Pb on Fe on Ir(111) is shown in Fig. 1(a), with two buried step edges of the Ir substrate indicated by the dotted lines. An area of the Fe double layer (Fe-DL) is labeled and the dislocation lines, which form due to strain relief [16], are visible. Whereas the first atomic layer of Fe on the Ir(111) is pseudomorphic, i.e., the lateral distances of the Fe atoms adapt to the Ir substrate, the second Fe layer releases some epitaxial strain by incorporating additional rows of atoms and thus forming dislocation lines running roughly along [11$\bar{2}$] directions. This results in a variation of the Fe adsorption site along [1$\bar{1}$0] alternating from fcc to hcp hollow sites with bcc-like areas in between [16]. The apparent height of a single atomic layer of Pb grown on the Fe-DL also reflects the dislocation lines; see the labeled elongated island in Fig. 1(a). The simultaneously measured dI/dU map in Fig. 1(b) shows a lower signal for the Fe-DL compared to the Pb/Fe-DL. On both areas, modulations of the signal are visible, which originate from local electronic differences due to the dislocation lines as well as the magnetic contrast due to spin-polarized tunneling.

The structure and magnetic state of the Fe-DL and the Pb/Fe-DL can be analyzed better in Fig. 2, which shows a closer view of a Pb monolayer island on the Fe-DL. In the topography image in Fig. 2(a), it becomes apparent that the dislocation lines continue from the Fe-DL to the Pb island, as indicated by the black lines. In the center of this Pb monolayer island, the distance between identical dislocation lines is roughly 6.5 nm. In the simultaneously recorded dI/dU image, shown in Fig. 2(b), a magnetic signal is visible both

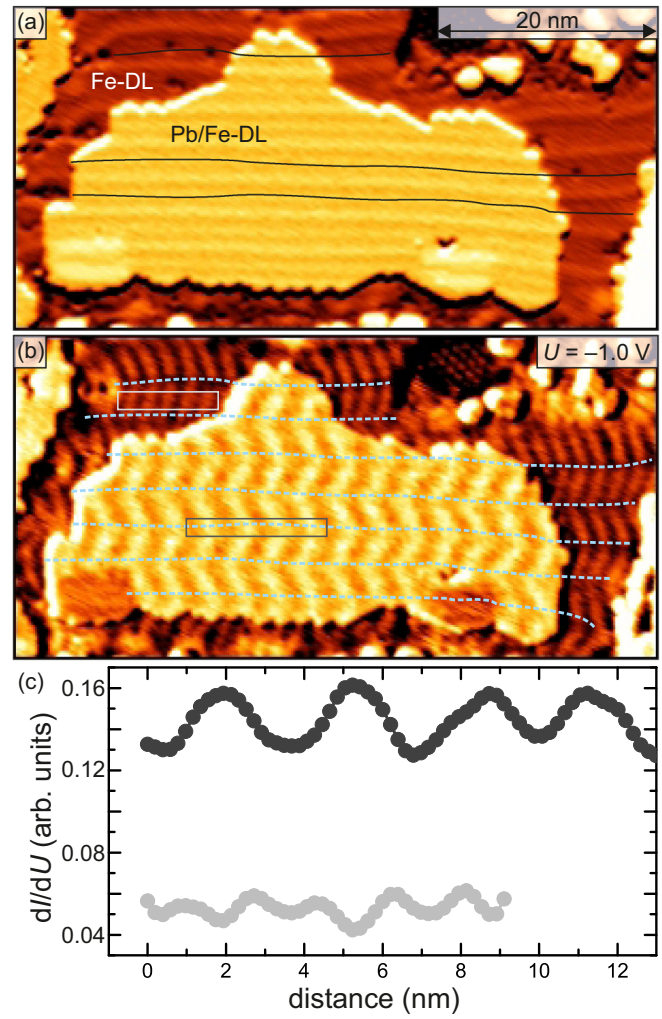

FIG. 2. (a) SP-STM measurement of a Pb island on the Fe-DL on Ir(111) (partially differentiated topography), showing the dislocation lines in the Fe-DL as well as in the Pb island. (b) Simultaneously acquired dI/dU signal, which exhibits a zigzag magnetic contrast both on the Fe-DL and the Pb/Fe-DL with different periods. The lines indicate the turning points of the zigzag pattern, which are at the same positions for the Fe-DL and the Pb/Fe-DL. Note that the darker dI/dU signal at the bottom left and bottom right of the Pb island originate from small islands of Fe instead of the Pb overlayer. (c) dI/dU line sections along the Pb/Fe-DL and the Fe-DL spin spirals taken at the positions indicated with the dark- and light-gray rectangles in (b), respectively. $U = -1$ V, $I = 1$ nA, $T = 4.2$ K.

for the Fe-DL as well as the Pb/Fe-DL. As reported previously [16], in the Fe-DL the dislocation lines guide a magnetic spin spiral along [11$\bar{2}$]; in this sample area, this spin spiral has a period of about 1.8 nm. It exhibits a zigzag-shape wave front due to the underlying atomic structure, and the kinks of the zigzag pattern are located at the lines of Fe atoms in fcc and hcp hollow sites. We also find a zigzag pattern on the Pb/Fe-DL, which propagates in the same direction as the one on the Fe-DL and also has the kinks on the same lines; see dashed lines in Fig. 2(b). We attribute this contrast to a spin-spiral state in the underlying Fe-DL. Whether or not the Pb itself is magnetically polarized cannot be derived from

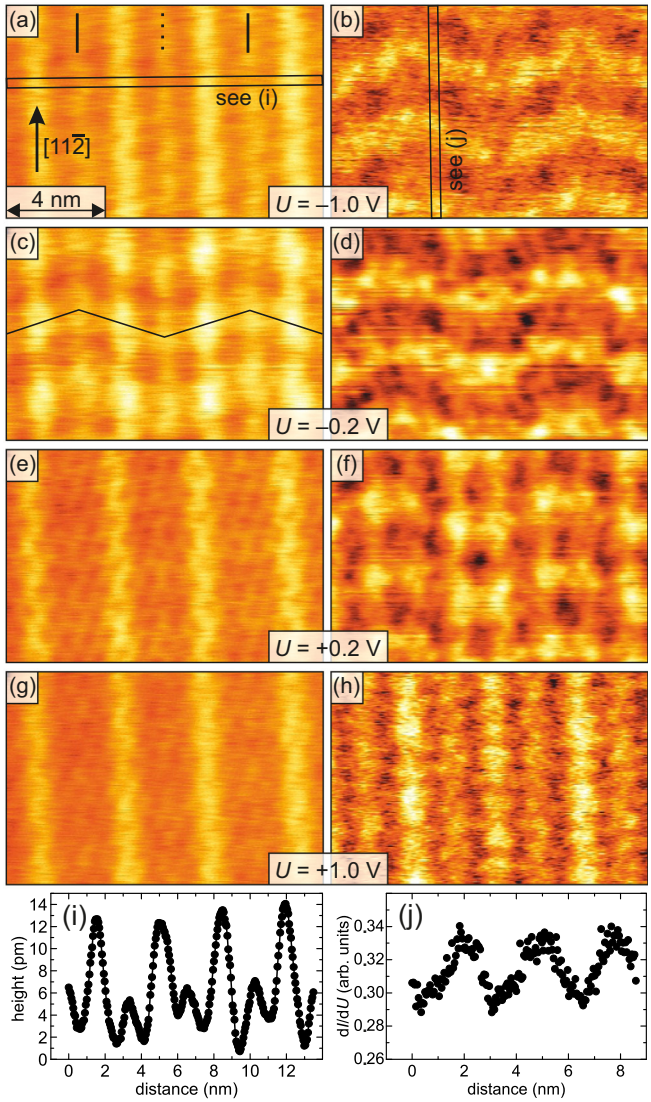

FIG. 3. Closer view of a Pb/Fe-DL area with (a),(c),(e),(g) topography images and (b),(d),(f),(h) simultaneously measured dI/dU maps. The applied bias voltage is varied and indicated in the images. Note that the topographic images are scaled to the same height difference. (i) and (j) are profiles along the rectangles shown in (a) and (b). $I = 1$ nA, $T = 4.2$ K. For the bias dependence of the uncovered Fe-DL, refer to Ref. [16].

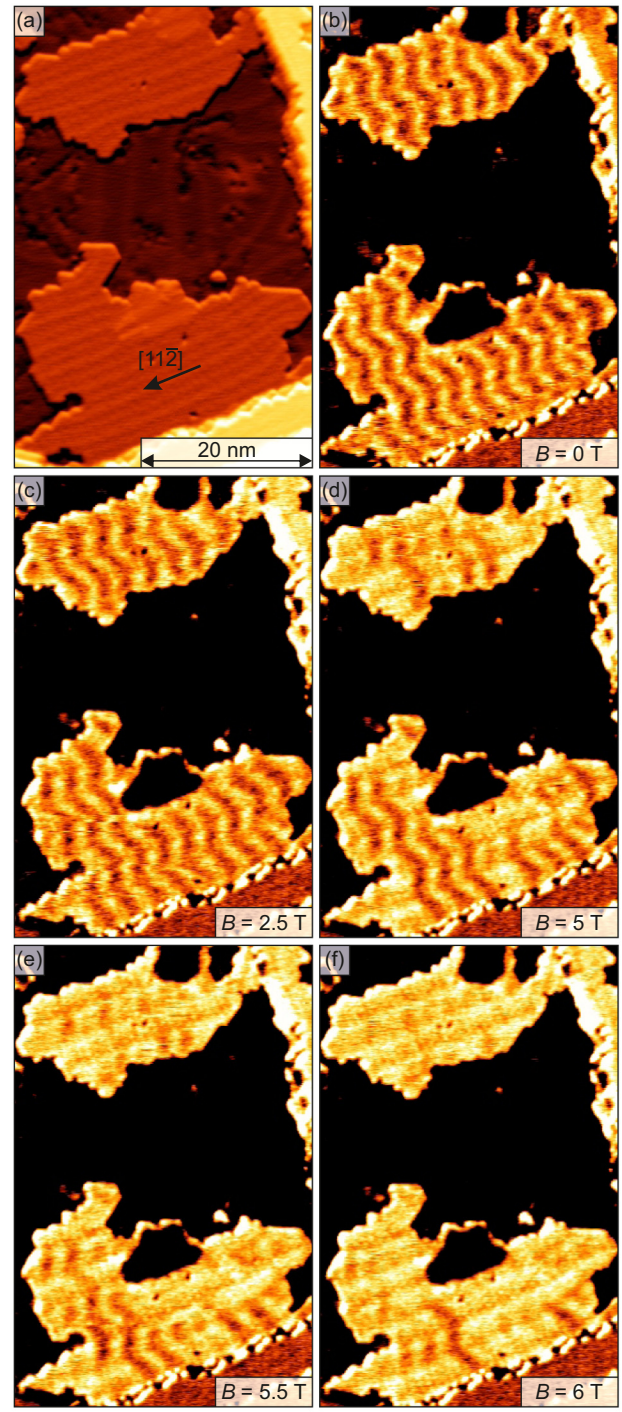

FIG. 4. (a) Topography of a sample area with two Pb islands on the Fe-DL (partially differentiated). (b)–(f) Corresponding spin-resolved dI/dU maps at different external magnetic fields B as indicated. With increasing B, the zigzag spin spiral on the Pb island vanishes, segment by segment. Note that the tip is unchanged throughout the series, and changes in the dI/dU signal reflect changes of the spin texture of the sample ($U = -1$ V, $I = 1$ nA, $T = 4.2$ K).

these experiments, but due to the closed d shell, we consider a large magnetic polarization of Pb unlikely. Note that a spin-polarized tunnel current can also occur when a monolayer of nonmagnetic atoms covers a magnetic material because the vacuum density of states can be highly spin polarized even when the surface atoms are nonmagnetic [22,23]. Figure 2(c) displays line profiles of the dI/dU signal along the two spin spirals of the Pb-covered and the uncovered Fe-DL taken at the positions indicated by the rectangles in Fig. 2(b). Measuring about 3.1 nm along [11$\bar{2}$], the periodicity of the spin spiral on the Pb/Fe-DL is nearly twice that of the uncovered Fe-DL.

Based on density-functional-theory calculations [12], the spin-spiral state of the Fe-DL on Ir(111) has been attributed to strongly frustrated exchange interactions, where the nearest-neighbor Heisenberg exchange J_1 is ferromagnetic and the next-nearest-neighbor exchange J_2 is antiferromagnetic with a ratio of 2:1 between them. The DMI selects the rotational sense, but because it is only 4% of the strength of J_1, it is of

minor importance for the small period length of the spin spiral in the Fe-DL. We find that the hybridization of the Fe-DL with the Pb leads to a strong increase of the spin-spiral period. Because of the large spin-orbit coupling of the Pb, one could argue that the effective DMI of the Fe film will be strongly affected due to the additional contribution from the Pb/Fe interface. However, because neither the strength nor the sign of the DMI at the Pb/Fe interface is known, predictions for the effective DMI, or whether an increase or decrease of the spin-spiral period is expected, are not possible. An alternative mechanism to induce a longer spin-spiral period is a larger ratio of J_1/J_2, for instance by an increase of J_1 or a quenching of J_2 due to the hybridization with the Pb overlayer.

Figure 3 shows a smaller area of the Pb/Fe-DL, measured at different bias voltages as indicated, with topography images in the left column and the corresponding dI/dU maps in the right column. Here, the dislocation lines are running vertically and, depending on the bias voltage, one can see in the topography two different alternating lines as in Fig. 3(a) or just one type of line as in Fig. 3(g). Here, the brighter lines visible at all displayed bias voltages can be correlated with bcc-like areas of the underlying Fe-DL, whereas the lines with smaller apparent height in Fig. 3(a) correspond to the alternating lines of Fe atoms in fcc and hcp hollow sites. Also, the amplitude of the magnetic signal depends strongly on the applied bias voltage and, in the topography, it is large at -0.2 V [Fig. 3(c)], whereas it is negligible for the other shown bias voltages. At positive bias voltages, a faint additional hexagonal superstructure of dark dots is visible, which is of structural origin. A close comparison of the position of the zigzag wave front with the position of the dislocation lines again demonstrates that the kinks of the wave front are located at the fcc and hcp stacked lines of the underlying Fe-DL. In this sample area, the distance between identical dislocation lines is 6.9 nm and the magnetic period along $[11\bar{2}]$ is 2.9 nm.

Figure 4(a) shows the topography of another sample with two Pb/Fe-DL areas, again appearing brighter in the corresponding dI/dU map in Fig. 4(b). Whereas the magnetic state of the uncovered Fe-DL remains unchanged in external magnetic fields (at least up to 9 T) [16], we observe an impact of the applied magnetic field on the zigzag spin spiral in the Pb/Fe-DL; see dI/dU maps in Figs. 4(b)–4(f), all measured with the identical tip. The magnetic field aligns the spin spiral segment by segment, starting between 2.5 and 5 T. While the magnetic state does not change between $B = 0$ T [Fig. 4(b)] and $B = 2.5$ T [Fig. 4(c)], clearly some parts of the spiral have vanished at $B = 5$ T [Fig. 4(d)]. With higher magnetic fields [Figs. 4(e) and 4(f)], the field-polarized area increases and, at $B = 6$ T [Fig. 4(f)], only a few fragments of the spiral are left. Not only the length scale and the zigzag shape of the spin spiral of the Pb/Fe-DL are reminiscent of the magnetic state in the Fe-TL on Ir(111), but also the qualitative magnetic field dependence with the stepwise disappearance of the spin spiral is similar [17,18]. Because in both cases the remaining spin-spiral segments are multiples of the dislocation line distance, we conclude that pinning of the magnetic texture to dislocation lines plays a role for this unusual magnetic field dependence. We find that the transition field for the Pb/Fe-DL of about 2.5–5 T is higher than the one of about 1–2 T for the Fe-TL, which we attribute at least in part to the smaller net magnetic moment in the Pb/Fe-DL. Because of the similarity to the Fe triple layer, where the magnetic objects induced by applied fields are distorted magnetic skyrmions [17], and because of the large DMI at the Fe/Ir interface, we also conclude that the spin-spiral segments in the Pb/Fe-DL represent topologically distinct magnetic skyrmions.

IV. CONCLUSION

We have shown that the magnetic state of a two-atomic-layer-thick Fe film on Ir(111) covered by a single atomic Pb layer is a spin spiral with a period of about 3 nm. This is about two times larger compared to the spin spiral without Pb. However, other properties such as the coupling of the propagation direction to the dislocation lines and the zigzag shape of the wave front of the spin spiral are common to both systems. Measurements in external magnetic fields have shown that in contrast to the uncovered Fe-DL, the Pb/Fe-DL reacts to external magnetic fields. At applied fields around 5 T, the spin spiral disappears segment by segment, and the observed magnetic objects are considered to represent magnetic skyrmions. This shows that a tuning of magnetic states by hybridization with additional metallic layers is not limited to transition metals, but that other materials such as Pb also can be used to tailor complex spin textures. We anticipate that a thicker Pb layer will not substantially change the properties of the Fe film, enabling the creation of an interface of superconducting Pb with a magnetic film that hosts a noncollinear spin texture.

ACKNOWLEDGMENTS

This project has received funding from the Deutsche Forschungsgemeinschaft (DFG, German Research Foundation) Grant No. SFB668-A8, and the European Unions Horizon 2020 research and innovation program under Grant Agreement No. 665095 (FET-Open project MAGicSky).

[1] N. Nagaosa and Y. Tokura, Nat. Nanotech. **8**, 899 (2013).
[2] K. von Bergmann, A. Kubetzka, O. Pietzsch, and R. Wiesendanger, J. Phys.: Condens. Matter **26**, 394002 (2014).
[3] R. Wiesendanger, Nat. Rev. Mater. **1**, 16044 (2016).
[4] A. Fert, N. Reyren, and V. Cros, Nat. Rev. Mater. **2**, 17031 (2017).
[5] S. Mühlbauer, B. Binz, F. Jonietz, C. Pfleiderer, A. Rosch, A. Neubauer, R. Georgii, and P. Boni, Science **323**, 915 (2009).
[6] X. Z. Yu, Y. Onose, N. Kanazawa, J. H. Park, J. H. Han, Y. Matsui, N. Nagaosa, and Y. Tokura, Nature (London) **465**, 901 (2010).
[7] G. Chen, T. Ma, A. T. N'Diaye, H. Kwon, C. Won, Y. Wu, and A. K. Schmid, Nat. Commun. **4**, 2671 (2013).

[8] B. Dupé, G. Bihlmayer, M. Böttcher, S. Blügel, and S. Heinze, Nat. Commun. **7**, 11779 (2016).

[9] A. Soumyanarayanan, M. Raju, A. L. Gonzalez Oyarce, A. K. C. Tan, M.-Y. Im, A. Petrovc, P. Ho, K. H. Khoo, M. Tran, C. K. Gan *et al.*, Nat. Mater. **16**, 898 (2017).

[10] S. Heinze, K. von Bergmann, M. Menzel, J. Brede, A. Kubetzka, R. Wiesendanger, G. Bihlmayer, and S. Blügel, Nat. Phys. **7**, 713 (2011).

[11] K. von Bergmann, M. Menzel, A. Kubetzka, and R. Wiesendanger, Nano Lett. **15**, 3280 (2015).

[12] P.-J. Hsu, L. Rózsa, A. Finco, L. Schmidt, K. Palotás, E. Vedmedenko, L. Udvardi, L. Szunyogh, A. Kubetzka, K. von Bergmann *et al.*, Nat. Commun. **9**, 1571 (2018).

[13] N. Romming, C. Hanneken, M. Menzel, J. E. Bickel, B. Wolter, K. von Bergmann, A. Kubetzka, and R. Wiesendanger, Science **341**, 636 (2013).

[14] N. Romming, H. Pralow, A. Kubetzka, M. Hoffmann, S. von Malottki, S. Meyer, B. Dupé, R. Wiesendanger, K. von Bergmann, and S. Heinze, Phys. Rev. Lett. **120**, 207201 (2018).

[15] D. Iaia, A. Kubetzka, K. von Bergmann, and R. Wiesendanger, Phys. Rev. B **93**, 134409 (2016).

[16] P.-J. Hsu, A. Finco, L. Schmidt, A. Kubetzka, K. von Bergmann, and R. Wiesendanger, Phys. Rev. Lett. **116**, 017201 (2016).

[17] P.-J. Hsu, A. Kubetzka, A. Finco, N. Romming, K. von Bergmann, and R. Wiesendanger, Nat. Nanotech. **12**, 123 (2017).

[18] A. Finco, P.-J. Hsu, A. Kubetzka, K. von Bergmann, and R. Wiesendanger, Phys. Rev. B **94**, 214402 (2016).

[19] M. Eschrig, Phys. Today **64**, 43 (2011).

[20] J. Li, T. Neupert, Z. Wang, A. H. MacDonald, A. Yazdani, and B. A. Bernevig, Nat. Commun. **7**, 12297 (2016).

[21] R. Wiesendanger, Rev. Mod. Phys. **81**, 1495 (2009).

[22] L. Berbil-Bautista, S. Krause, T. Hänke, M. Bode, and R. Wiesendanger, Surf. Sci. Lett. **600**, L20 (2006).

[23] L. V. Dzemiantsova, M. Karolak, F. Lofink, A. Kubetzka, B. Sachs, K. von Bergmann, S. Hankemeier, T. O. Wehling, R. Frömter, H. P. Oepen, A. I. Lichtenstein, and R. Wiesendanger, Phys. Rev. B **84**, 205431 (2011).